JOURNAL OF GEOPHYSICAL RESEARCH: SOLID EARTH, VOL. 118, 1471–1482, doi:10.1029/2012JB009582, 2013

# Influence of subglacial conditions on ice stream dynamics: Seismic and potential field data from Pine Island Glacier, West Antarctica

Andrew M. Smith, Tom A. Jordan,[1] Fausto Ferraccioli,[1] and Robert G. Bingham[2]

Received 28 June 2012; revised 5 November 2012; accepted 6 November 2012; published 15 April 2013.

[1] We interpret seismic reflection and airborne potential field data acquired on Pine Island Glacier, West Antarctica and find variations in the subglacial geology which correlate with variations in ice dynamics. Immediately beneath the glacier is a mixture of soft, deforming sediments and harder, non-deforming sediments. Beneath this, a sedimentary basin lies under part of the main glacier, with another under one of its slower-moving tributaries. A tectonic boundary underlies the main trunk of the glacier separating these sedimentary basins to the north from crystalline rocks to the south, which also include a thick, rift-related magmatic intrusion. The boundary correlates with changes in the basal roughness, ice flow speed, and basal drag. Smoother bed, faster flow, and lower basal drag characterize the thicker sedimentary sequences, to the north, but there is no corresponding lateral change in the acoustic properties of the bed. Changes in the sub-bed (i.e., deeper than the ice-bed interface) lithology appear to account for the contrasting basal drag and ice velocity patterns over the glacier. Subglacial erosion could remove a thin layer of soft sediments to the south of the geological boundary, leading to increased basal drag and reduced ice flow in the future. We conclude that the subglacial geology plays a significant role in controlling the spatial pattern of present-day ice flow and that the consequences of subglacial erosion may be reflected in temporal changes to the ice dynamics in the past and perhaps also in the near future.

**Citation:** Smith, A. M., T. A. Jordan, F. Ferraccioli, and R. G. Bingham (2013), Influence of subglacial conditions on ice stream dynamics: Seismic and potential field data from Pine Island Glacier, West Antarctica, *J. Geophys. Res. Solid Earth*, *118*, 1471–1482, doi:10.1029/2012JB009582.

## 1. Introduction

### 1.1. Basal Controls on Ice Stream Flow

[2] The majority of ice discharge to the sea from the Antarctic Ice Sheet is through fast-moving ice streams [*Bamber et al*., 2000; *Rignot et al*., 2008]. Understanding the basal controls on ice stream flow is important for modeling present and future ice sheet behavior [e.g., *Vaughan and Arthern*, 2007]. A physically based understanding (rather than simple parameterizations) of the basal boundary of glaciers is still lacking, but will be required for predictions of future ice sheet evolution to be realistic under changing climatic and oceanic forcing. Geophysical surveys have indicated that the presence of subglacial sediments is likely to be important in facilitating streaming flow and is possibly a critical controlling factor in determining the onset regions of several Antarctic ice streams. The location of a basin with sedimentary substrate, determined from airborne gravity and magnetic surveys, was found to correlate with the onset of Whillans Ice Stream (Ice Stream B) [*Bell et al*., 1998], and the edge of another basin, determined by seismic refraction, corresponds closely with the edge of Kamb Ice Stream (Ice Stream C) [*Anandakrishnan et al*., 1998]. Seismic reflection and refraction surveys have suggested that laterally continuous subglacial sediments are a necessary component for ice streaming in the onset and upstream regions of both the Kamb and Bindschadler Ice Streams (Ice Streams C and D) [*Peters et al*., 2006]. Aeromagnetic data have also indicated that a tributary of Slessor Glacier in East Antarctica is underlain by a thick sedimentary substrate [*Bamber et al*., 2006; *Shepherd et al*., 2006]. In this paper, we use the term "sediments" for all unlithified sedimentary material beneath the ice. These may include both materials whose presence is due to the ice (i.e., till) and some which are unrelated to the ice (possible former marine sediments, for example).

[3] Whilst the basal boundary is believed to be a critical control on ice stream flow, its exact nature is poorly understood. One technique that has been shown to provide information on this boundary is seismic reflection, from which the relative strength of the material at the glacier bed can be inferred [*Smith*, 1997a, 2007]. Generally, softer deforming sediments can be distinguished from harder non-deforming sediments and rock by their acoustic impedance values, determined from reflection strength. The presence of water can also be detected by this method [*King et al*., 2004]. In this paper, we present the first analysis of

[1]British Antarctic Survey, Cambridge, UK.
[2]School of Geosciences, University of Aberdeen, Aberdeen, UK.

Corresponding author: A. M. Smith, British Antarctic Survey, Cambridge, UK. (amsm@bas.ac.uk)


2169-9356/13/2012JB009582

seismic reflection profiles acquired on Pine Island Glacier, West Antarctica. We calculate the basal acoustic impedance and use this, along with airborne gravity and magnetic data, to interpret the shallow-medium depth subglacial geological structure and examine how the local geology affects the ice flow and its variability.

### 1.2. Pine Island Glacier

[4] Pine Island Glacier (PIG; Figure 1) is a large ice stream that drains 10% of the West Antarctic Ice Sheet (WAIS) [*Shepherd et al*., 2001]. In recent decades, PIG has undergone significant changes including grounding line retreat, acceleration, and thinning [e.g., *Rignot*, 1998; *Shepherd et al*., 2001; *Rignot et al*., 2002], with rates of acceleration and thinning increasing over the last decade [*Rignot*, 2008; *Scott et al*., 2009; *Wingham et al*., 2009]. Recent airborne radar, gravity, and magnetic data collected across the PIG catchment provided insights into the subglacial topography and underlying geological structures that may represent important boundary conditions for ice dynamics [*Vaughan et al*., 2006; *Ferraccioli et al*., 2007a; *Jordan et al*., 2010]. The main trunk of the ice stream is situated in a 250 km long, 500 m deep subglacial trough. Two tributaries lie in similar troughs, whereas other tributaries occupy poorly defined, shallow bed depressions [*Vaughan et al*., 2006]. Gravity data indicate that the trough along which the main trunk flows overlies a crustal-scale rift [*Jordan et al*., 2010]. Previous studies have attempted to determine the basal conditions of PIG over the whole ice stream using airborne and satellite data. They report mixed conditions suggesting areas of both bedrock and weak sediment [*Joughin et al*., 2009; *Morlighem et al*., 2010].

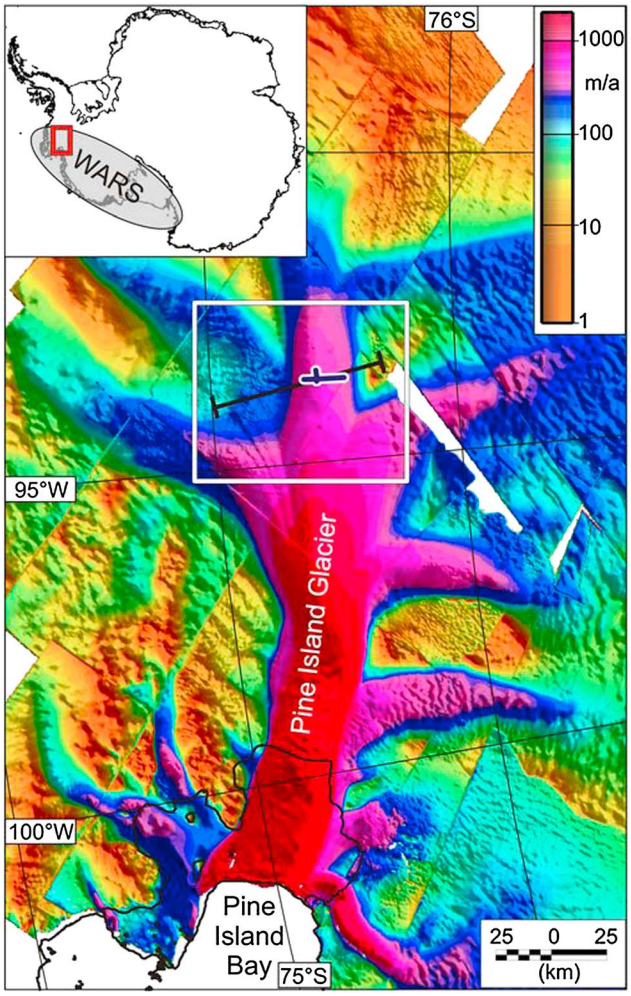


**Figure 1.** Location map of Pine Island Glacier. Background shows ice velocity derived from InSAR measurements [*Joughin et al*., 2003]. The white box marks zoomed area in Figure 2. Within the white box, a black line marks the segment of the airborne survey flight line used for the potential field model; seismic survey lines are marked in blue with a white border. The inset shows the Antarctic context of the map (red box) along with the area of the West Antarctic Rift System (WARS) [e.g., *Bingham et al*., 2012].

## 2. Methods

### 2.1. Seismic Reflection Data

#### 2.1.1. Data Acquisition and Processing

[5] During December 2007, two seismic reflection lines were acquired on PIG (Figures 1 and 2), an 18 km line aligned perpendicular to ice flow and a 5 km line aligned along the flow. The seismic source was 300 g of high explosive at the bottom of a 20 m hole, drilled with hot water and backfilled. Shots were spaced at 240 m intervals and reflections were detected by 48 vertically orientated 100 Hz geophones at 10 m spacing, out to a maximum offset of 500 m. Data were recorded at a sampling interval of 0.125 ms. This acquisition geometry produces single-fold coverage with a reflection-point spacing of 5 m at the bed. Maximum incident angles were ~7° so the data can be considered effectively normal incidence. At three selected locations larger, 2 kg shots were also fired so that the first multiple reflection from the ice-bed interface could be recorded. This allowed the bed reflection coefficient to be calibrated [*Smith*, 1997a, 2007]. Shallow seismic refraction surveys were used to determine the seismic velocity in the upper ~200 m of the glacier, with first arrivals being measured at offsets up to 1 km [e.g., *Kirchner and Bentley*, 1990].

[6] Data were corrected for shot depth. A normal moveout (NMO) correction was applied to account for varying geophone offset from the source. Predictive deconvolution was used to remove reflections from source energy traveling up and reflecting off the air-snow surface giving a ghost reflection ~20 ms after each primary one. Finally, a Kirchhoff migration was used to collapse hyperbolae and to position reflectors correctly. A band-pass filter was applied for display purposes only, not for determining bed reflection strength.

#### 2.1.2. Acoustic Impedance

[7] The basal reflection coefficient was determined following the method of *Smith* [1997a, 2007]. The relationship between the energy of the primary and first multiples is given in terms of the reflection coefficient, $R$, for normal incidence as

$$\frac{E_1}{E_2} = \frac{4}{R^2} e^{2ah}, \tag{1}$$

where $E_1$ and $E_2$ are the wavelet energies for the basal reflection and its first multiple respectively, $a$ is the attenuation coefficient, and $h$ is the ice thickness [*Roethlisberger*, 1972]. An attenuation coefficient in the ice, $a$, (defined in terms of

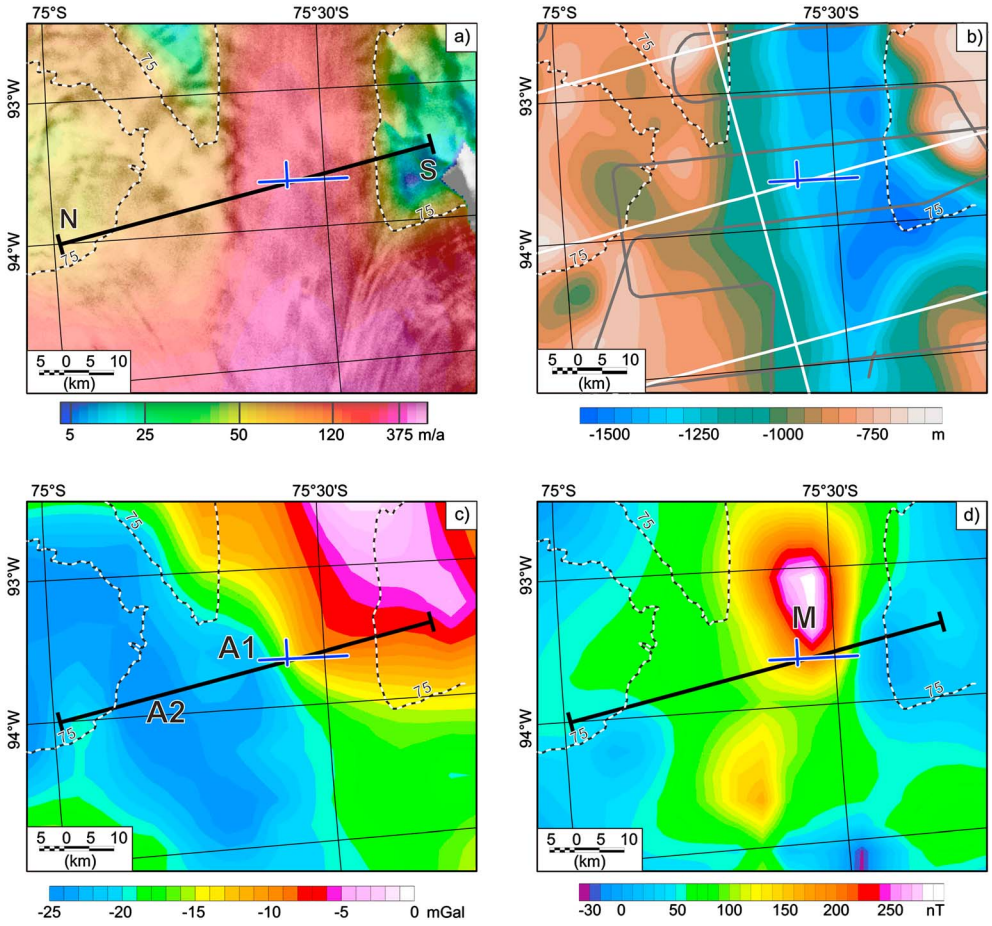


**Figure 2.** Survey area maps. Seismic survey lines are marked in blue with a white border; bold black line marks the segment of the airborne survey flight line used; thin black lines are the graticule. The black and white line marks the 75 m a$^{-1}$ flow speed contour. (a) Ice velocity from InSAR measurements [*Joughin et al.*, 2003] shaded with a RADARSAT image to show ice stream shear margins. (b) Sub-ice elevation derived from airborne radar data [*Vaughan et al.*, 2006]. White lines mark flights where airborne radar, gravity, and magnetic data were collected. Grey lines show flights where only radar and magnetic data were collected. Note offset of fastest flowing ice from deepest topographic trench. (c) Airy isostatic gravity anomaly map. A1 and A2 mark local gravity lows. (d) Magnetic anomaly map. M marks a positive magnetic anomaly.

energy) of $4 \pm 1 \times 10^{-4}$ m$^{-1}$ was used, for this region, based on the most comparable studies in terms of temperature range [*Robin*, 1958; *Brockamp and Kohnen*, 1965; *Bentley*, 1971; *Bentley and Kohnen*, 1976; *Smith* 1997a; *Holland and Anandakrishnan*, 2009].

[8] The bed reflection coefficient at other points was then calculated using these values from the multiple reflections for reference:

$$R^2 = \frac{R_m^2 E_1 h^2}{E_{1m} h_m^2} e^{2a(h-h_m)}, \quad (2)$$

where the subscript, $m$, denotes the values at the location where the multiple was recorded [*Smith*, 1997a]. The basal acoustic impedance, $Z_b$, was then calculated from

$$Z_b = Z_i \frac{(1+R)}{(1-R)}, \quad (3)$$

where $Z_i$ is the impedance of the ice, taken as $3.33 \pm 0.04 \times 10^6$ kg m$^{-2}$ s$^{-1}$ [*Atre and Bentley*, 1993].

## 2.2. Airborne Gravity and Magnetic Data

[9] An aerogeophysical survey was conducted over PIG in 2004/05 [*Vaughan et al.*, 2006], acquiring simultaneous gravity, magnetic, and radar data (Figure 2). A summary of the aerogravity data and a crustal interpretation were given by *Jordan et al.* [2010]. The gravity data were smoothed with a 9 km half-width, space domain, kernel filter [*Holt et al.*, 2006]. A Bouguer correction was applied, and an Airy isostatic model was removed, to account for the regional effect of crustal thickness variations. The 265 crossover points gave a standard deviation of 2.8 mGal. The data reveal a change from locally positive Airy isostatic residual anomalies south of PIG to more negative anomalies toward the northwest (Figure 2c). Processing steps applied to the raw magnetic data included magnetic compensation for aircraft motion, diurnal correction, International Geomagnetic Reference Field correction, statistical leveling [*Ferraccioli et al.*, 2007b], and microleveling in the frequency domain, to minimize residual line-related noise [*Ferraccioli et al.*, 1998]. The microleveled

magnetic anomaly data were then draped [*Pilkington and Thurston*, 2001] to a height of 2700 m over the subglacial topography [*Vaughan et al*., 2006]. This drape interval was chosen to be equal to the mean distance between the flight elevation and the bedrock over the entire catchment of PIG. For the draping correction, we used the profile radar and magnetic data as opposed to gridded data, as in other surveys over deep subglacial basin regions [*Ferraccioli et al*., 2009]. Final crossover errors for the microleveled, draped magnetic anomaly data for the PIG region were ~3 nT.

[10] We used 2-D forward modeling (Geosoft GM-SYS$^{TM}$) to analyze the possible geological sources of the Airy isostatic and magnetic anomalies along a flight line, which intersects the seismic lines described above (Figures 1 and 2). None of the data processing applied changed the location of the potential field anomalies, so the gravity and magnetic data can be interpreted together. However, as the gravity data were smoothed, whereas the magnetic data were not, we do not attempt to compare potential field anomaly gradients.

### 2.3. Ice Flow Speed

[11] The surface ice-flow speed at points along the seismic line was measured by recording the positions of the shot points using GPS receivers at the beginning and end of a 25 day period in December 2007. This is presented in Figure 3, along with the speed from InSAR measurements taken in 1996 [*Joughin et al*., 2003]. Figure 3 shows that the seismic line is located across the central flow region of the ice stream and that the flow speed across this region had increased by an average of 35% since 1996. At this location the flow maximum is not located in the deepest part of the bed trough [*Vaughan et al*., 2001].

## 3. Results and Interpretation

### 3.1. Seismic Reflection Profiles

#### 3.1.1. Results

[12] The processed seismic reflection sections are shown in Figures 4 and 5 and some reflecting horizons have been picked. The ice stream bed can be clearly delineated in both across- and along-flow sections, and some englacial reflections are present. Primary reflections can also be picked below the ice stream bed, most notable of which is a dipping band of arrivals marked in red in Figures 4 and 5. The same feature can be identified on both sections, from its character and from the fact that it arrives at the same travel time at the intersection of the two profiles. In the area to the north of the dipping reflection the bed has a degree of acoustic transparency, and sub-basal reflections can be distinguished. A more horizontal reflector, shown in blue, is also seen in both lines above the dipping reflector. Other sub-basal reflections are shown in black but cannot be linked between the two profiles. No coherent sub-bed arrivals can be picked to the south of the dipping reflection.

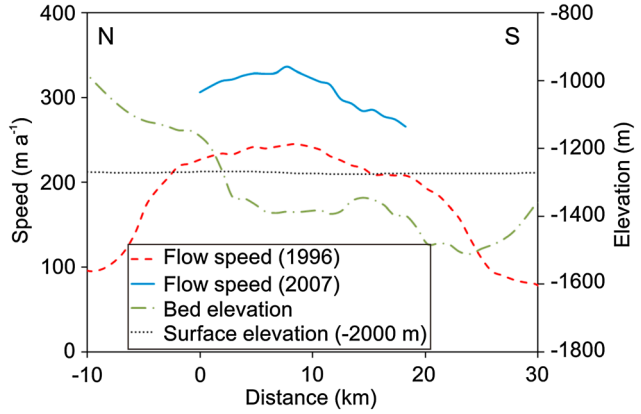


**Figure 3.** Ice surface flow speed along the across-flow seismic line (blue) compared with the 1996 flow speed from InSAR (red) [*Joughin et al*., 2003]; ice stream bed elevation from *Vaughan et al*. [2006]; ice surface elevation from *Bamber et al*. [2009] with 2000 m subtracted to display it on the same axis as the bed elevation. Flow direction is out of page.

#### 3.1.2. Acoustic Impedance Results

[13] The acoustic impedance of the bed was calculated for the whole of the along-stream line and most of the across-stream line (Figure 6). In areas where the bed reflection strength could not be determined, usually due to processing artifacts, the results are not displayed. The values given in Figure 6 are averages over ~100 m of bed (approximately the radius of the first Fresnel zone) to remove any isolated spikes in the data. The results show that the majority of the bed in this area comprises soft, water-saturated deforming sediments, with some areas of harder non-deforming sediment, and possibly some areas of water (Figure 6). From seismic measurements, similar mixed beds have also been described on Rutford Ice Stream, Talutis Inlet, and Bindschadler Ice Stream (Ice Stream D) [e.g., *Smith*, 1997c; *Vaughan et al*., 2003; *King et al*., 2004; *Peters et al*., 2006; *Smith and Murray*, 2009].

#### 3.1.3. Interpretation of Seismic Reflections

[14] To place the reflectors at the correct elevation, the seismic velocities are needed. The shallow refraction measurements gave a mean seismic velocity down to 150 m depth of 3226 m s$^{-1}$ and, at this depth, a velocity of 3800 ± 20 m s$^{-1}$. A correction was made for the increase in ice temperature toward the ice base, assuming the velocity decreases linearly over the lower 500 m from 3800 to 3750 m s$^{-1}$. We also made a correction for the 20 m shot depth, based on the velocity obtained from the shallow refraction. The surface elevation was obtained from the GPS measurements at the shot points.

[15] Seismic wave speed is more difficult to determine below the base of the ice. In the acoustically transparent area where sub-basal reflectors have been picked, the ice stream bed has an average acoustic impedance of $2.93 \times 10^6$ kg m$^{-2}$ s$^{-1}$. A compilation of published data on sediments in Antarctica by *Smith* [1997b] suggests a density of around 1750 kg m$^{-3}$ and a seismic velocity of around 1675 m s$^{-1}$; however, this is only for the sediments immediately beneath the ice which, for an acoustic impedance this low, are likely to be highly porous, deforming sediments. These values are therefore lower limits for the velocity and density of the sub-basal material. The fact that we can clearly see primary returns at two-way travel times of up to 240 ms below the bed suggests there is no strong impedance contrast between the ice stream bed and the observed sub-basal reflectors and that there is reasonable transmission. Therefore, it is likely that this area consists of soft sediments or sedimentary rock, for which a velocity range between 1675 and 2500 m s$^{-1}$ is reasonable [*Telford et al*., 1990; *Smith*, 1997b]. As the bed

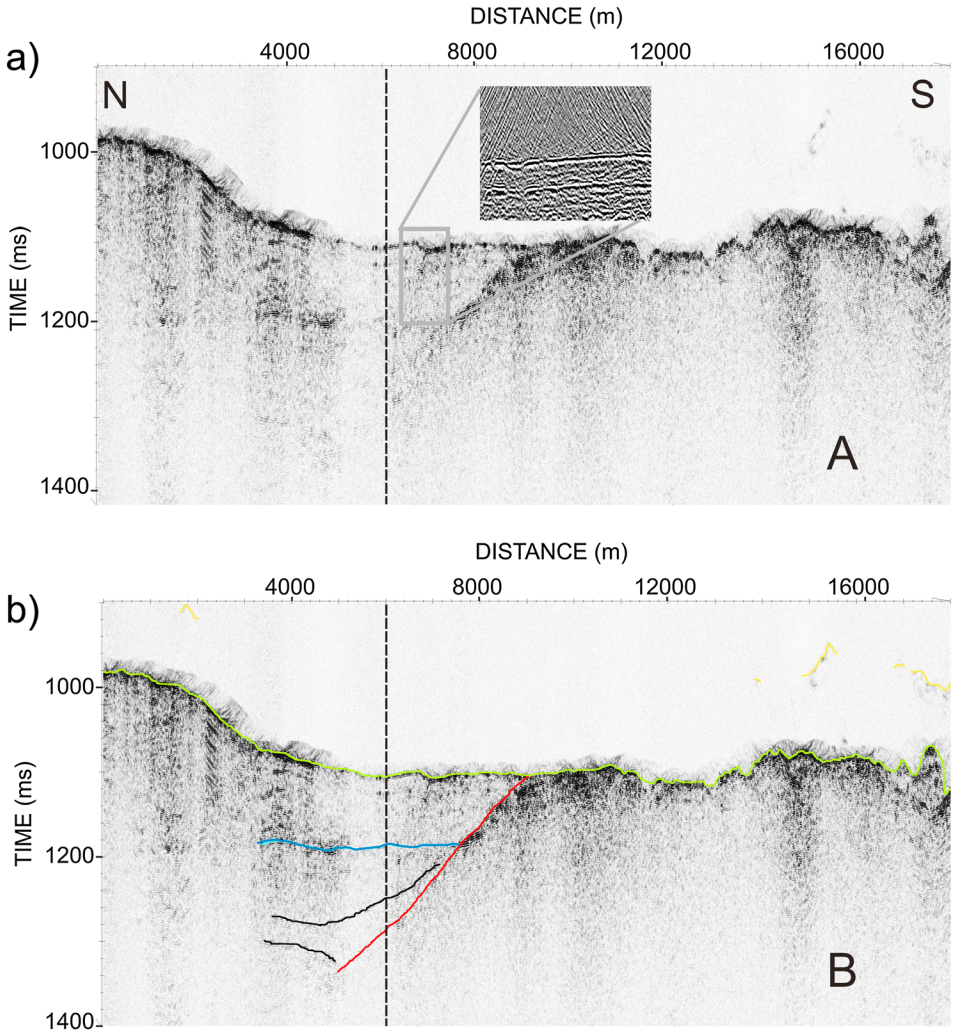


**Figure 4.** Processed across-stream seismic section. Ice flow is out of the page. Position of along-stream line is marked by dashed line. (a) Uninterpreted section. (b) Interpreted section showing selected picked reflecting horizons: green, ice stream bed; yellow, englacial reflectors; red and blue, sub-basal reflecting horizons that can be identified in both the along-stream and across-stream lines; and black, other sub-basal horizons. Inset in Figure 4a illustrates the quality of the ice-bed interface reflection, justifying its use in determining reflection strength.

of the ice stream is likely to be at the lower end of this range, we estimate an average sub-basal velocity of 2000 m $s^{-1}$ and plot the corresponding reflector elevations in Figure 7.

[16] With the support of potential field data presented in the next section, we interpret the band of dipping reflectors (red line in Figures 4, 5, and 7) as a major geological boundary, with layers of sedimentary infill (sediments and/or sedimentary rocks) above (blue and black lines). Between 0 and 3 km (Figure 7a), the sub-basal reflections cannot be traced clearly. This may be due to the absence of continuous sub-basal reflectors in this area or to the higher reflectivity of the ice stream bed. Given the likely velocity range in sediments, we determined the strike of the geological boundary to be ~040° with a dip of approximately 4° to the NW.

### 3.2. Potential Field Results

#### 3.2.1. Gravity Model

[17] The Airy isostatic anomaly map (Figure 2c) shows a distinct inflection, coincident with the location and strike of the geological boundary identified from the seismic data. This inflection can also be seen clearly in Figure 8b where a 15 mGal step is evident. To model this, we introduced a layer of lower density material in the north (2400 kg $m^{-3}$) compared to the south (2670 kg $m^{-3}$). This layer may represent lithified sediments infilling the northern part of the PIG rift [*Jordan et al.*, 2010]. The thickness of this layer (around 1.2 km) was estimated by fitting the amplitude of the longer wavelength Airy isostatic anomaly. Even after introducing this layer, shorter wavelength, negative anomalies remained along the northern part of the profile, which we modeled as low density material (1900 kg $m^{-3}$) up to 800 m thick (Figure 8). This is consistent with the seismic estimates of very low densities at the ice/bed interface (minimum 1750 kg $m^{-3}$) and would be typical of unconsolidated sediment overburden [e.g., *Telford et al.*, 1990]. However, the amplitudes of the shorter wavelength anomalies are close to the RMS error for the airborne gravity data (~3 mGal) and hence the thickness of the upper sedimentary layer is poorly constrained.

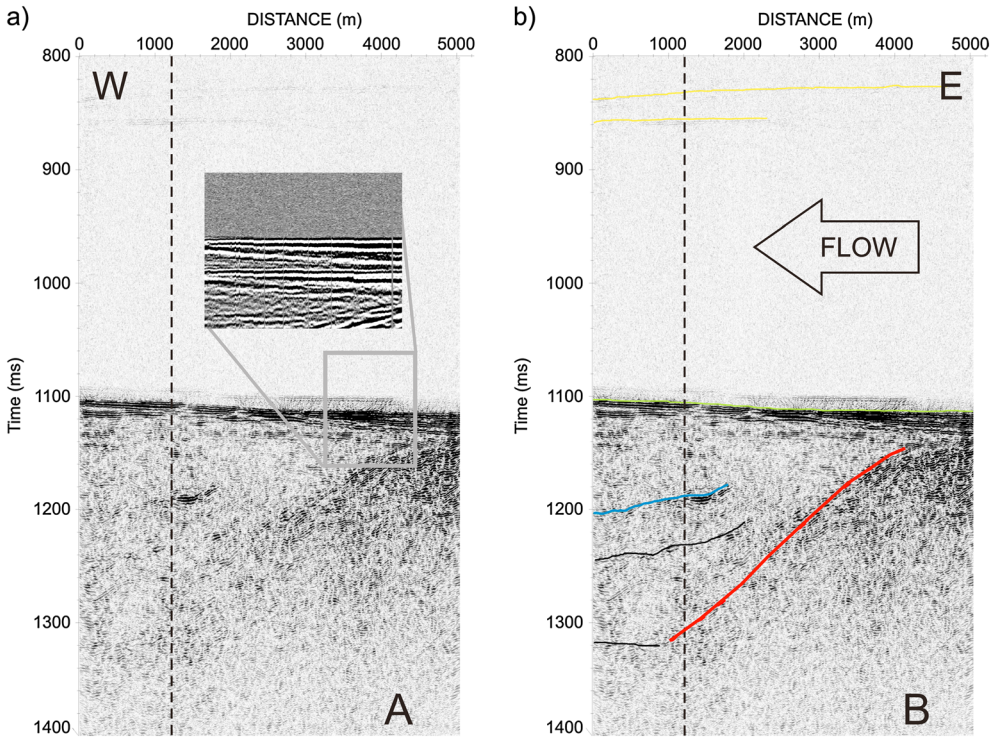


**Figure 5.** Processed along-stream seismic section. Ice flow is from right to left. Position of across-stream line is marked by dashed line. (a) Un-interpreted section. (b) Interpreted section showing selected picked reflecting horizons: green, ice stream bed; yellow, englacial reflectors; red and blue, sub-basal reflecting horizons that can be identified in both the along-stream and across-stream lines; and black, other sub-basal horizons. Inset in Figure 5a illustrates the quality of the ice-bed interface reflection, justifying its use in determining reflection strength.

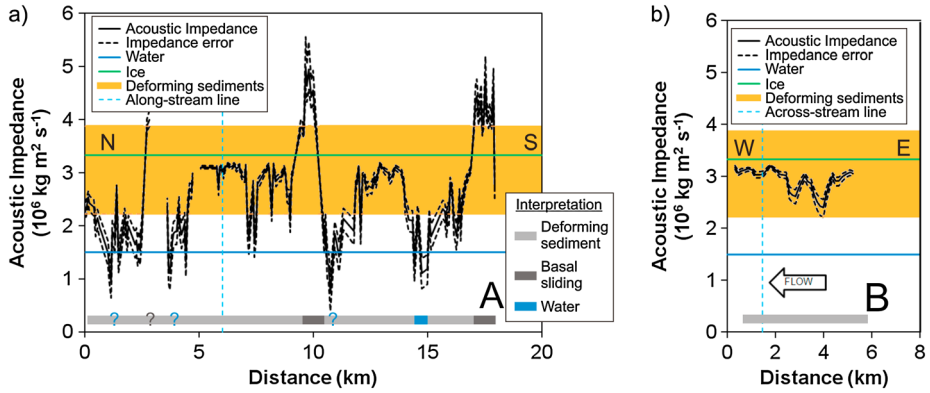


**Figure 6.** Acoustic impedance calculated from the seismic reflection surveys. Error bounds show the range due to uncertainty in the attenuation factor. The acoustic impedance of ice and water are given, along with an orange shaded region showing the acoustic impedance range expected for dilated, water-saturated deforming sediments [*Atre and Bentley*, 1993; *Smith* 1997a]. Interpretation of the basal conditions is also given. (a) Across-stream; ice flow is out of the page. (b) Along-stream.

### 3.2.2. Magnetic Model

[18] Magnetic data across the main trunk of PIG show a strong positive anomaly (labeled M in Figure 8), associated with the region of fastest ice flow (Figures 2d and 8a), and our survey line crosses the edge of this peak (Figure 2d). Modeling indicates that an intrusive body close to or at the ice-bed interface can account for this anomaly. This agrees with results of Werner deconvolution [*Ku and Sharp*, 1983], which reveals clusters of "contact" solutions close to the ice-bed interface, bracketing the magnetic high, along the southern flank of the sedimentary basin inferred from the seismic and gravity data.

[19] Our model shows that a ~2.5 km thick, 10 km wide magnetic body with an apparent susceptibility of 0.05 (SI units) can fit the observed anomaly. The thickness of the intrusion depends on the apparent susceptibilities used

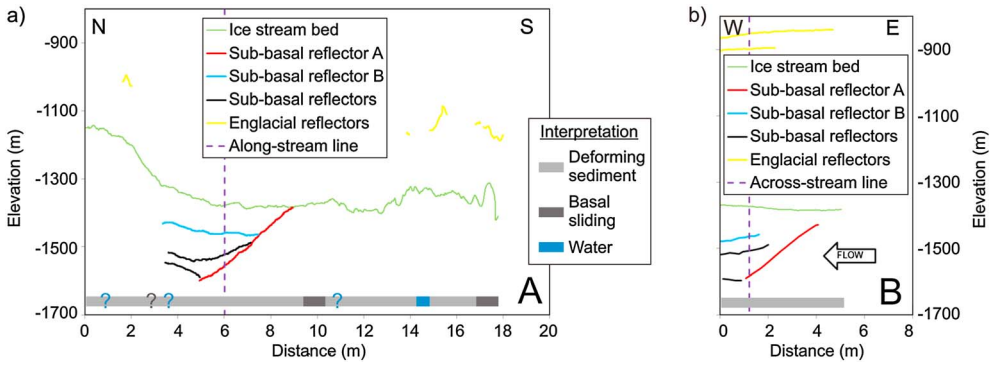


**Figure 7.** Depths of reflectors picked from seismic sections, assuming a sub-basal velocity of 2000 m $s^{-1}$. Interpretation of basal conditions from Figure 6 is also shown. (a) Across-stream; ice flow is out of the page. (b) Along-stream.

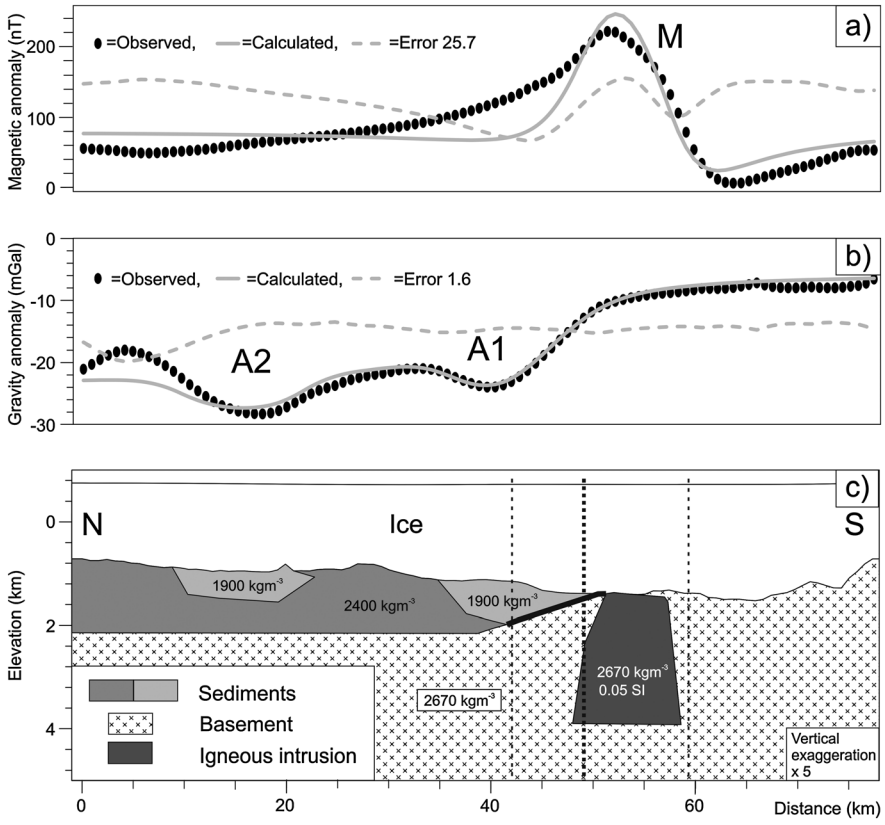


**Figure 8.** Potential field 2D forward models across PIG. (a) Aeromagnetic anomaly data and model. Positive anomaly is marked M. (b) Airy isostatic gravity anomaly data and model. Local gravity lows are marked A1 and A2. (c) Object-orientated model used to fit the anomalies shown in Figures 8a and 8b. Thin vertical dotted lines mark extent of seismic data. Thick vertical dotted line marks intersection with along-flow seismic line. Bold, diagonal solid line marks dipping interface extrapolated from seismic results. Annotated values in kg $m^{-3}$ refer to rock/sediment density; the modeled igneous intrusion has a magnetic susceptibility of 0.05 SI.

in the model. High values such as those in our model are typical of Cenozoic magmatic rocks related to the West Antarctic Rift System (Figure 1), and the considerable thickness of the intrusion is comparable with that proposed by *Behrendt et al*. [1994] for similar magnetic anomalies over the Siple Coast ice streams. There is no corresponding gravity high over the magnetic anomaly, and consequently our model shows no apparent density contrast over the intrusion. However, considering its relatively narrow width and the spatial filtering applied, the intrusion may simply be too small at this location to be resolved by our airborne gravity data. Hence, even though our model does not show a density contrast, it remains possible that one does exist in the subsurface geology.

#### 3.2.3. Potential Field Data Interpretation

[20] Our interpretation of the potential field data suggests that this part of PIG flows along a major tectonic contact juxtaposing denser crystalline basement to the south and sedimentary basins to the north. Close to this inferred tectonic boundary are areas of low density, unconsolidated sediments. An approximately 2.5 km thick and 10 km wide magnetic intrusion underlies the trunk of PIG (Figure 8c). We interpret the intrusion as the sub-volcanic roots of a Cenozoic magmatic complex associated with the inferred Pine Island Rift [*Jordan et al*., 2010]. We propose that a pre-existing rift-related fault zone underlying the glacier may have become leaky, facilitating emplacement of the magmatic complex. Similar interpretations have been made for Cenozoic intrusions in the Ross Sea Rift region [*Ferraccioli and Bozzo*, 2003]. Erosion of the overlying volcanic edifice has been proposed for the majority of Cenozoic magmatic complexes inferred to underlie fast flowing parts of WAIS [e.g., *Behrendt et al*., 1994] and would be likely for the trunk of PIG. Alternative interpretations relating the magnetic intrusion to Jurassic rift-related granitoids, exposed in the Weddell Sea region [*Jordan et al*., 2012], or older Paleozoic intrusions [*Ferraccioli et al*., 2002] outcropping in Marie Byrd Land, are less likely, as these rocks are typically marked by considerably lower amplitude magnetic anomalies.

### 3.3. Synthesis with Bed Roughness, Ice Velocity, and Basal Drag

[21] It has been suggested that soft sediments can bury rough bedrock features, smoothing the ice-bed interface and facilitating enhanced basal sliding [*Anandakrishnan et al*., 1998; *Bingham and Siegert*, 2009; *Li et al*., 2010; *Rippin et al*., 2011]. Figure 9 shows the bed elevation from the across-stream seismic line with a 1 km running mean subtracted, leaving only variations with a wavelength of approximately the ice thickness, or less. Basal roughness increases at around 9–10 km along the profile. This can be quantified using the standard deviation (σ), which increases from 3.4 m (0–9 km) to 13.5 m (9–18 km). An increase in roughness can be seen at a similar point in a nearby profile shown in Figure 3b of *Rippin et al*. [2011]. This location coincides with the interpreted sub-bed, geological boundary between low density sediments to the north and denser basement rocks to the south (Figure 8).

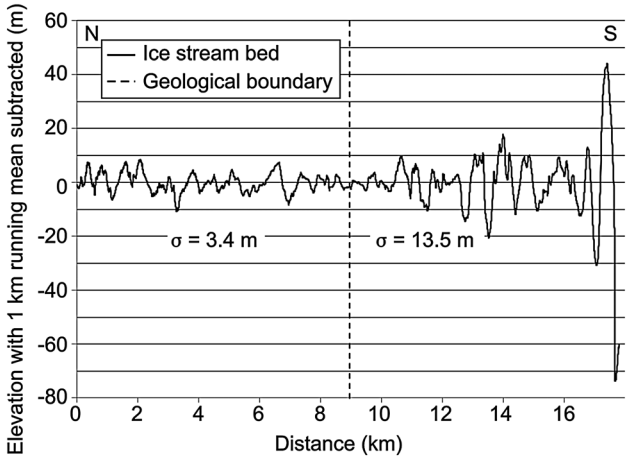


**Figure 9.** Ice stream bed elevation from across-stream seismic profile (Figure 4) with a 1 km running mean subtracted.

[22] Coincident with the increase in bed roughness and the sub-bed geological boundary, there is also a reduction in the ice flow speed from 325 to 290 m $a^{-1}$ (mean values; Figure 3). Additionally, modeling also suggests a corresponding increase in basal drag; spatial patterns of basal drag were inferred for PIG by *Morlighem et al*. [2010] using a full-Stokes ice-dynamics model. Data provided by M. E. Morlighem et al. (personal communication, 2010; a high-resolution version of Figure 2a in *Morlighem et al*. [2010]) demonstrate that there is generally low basal drag under the ice stream. However, there is an increase in basal drag southward across the geological boundary. Under the northern part of the ice stream with the lower basal roughness (Figure 9), the mean inferred basal drag is 3.4 kPa. This increases sharply across the boundary with a mean of 7.8 kPa on the rougher side to the south. We therefore find a coincidence between transitions in ice flow speed, basal roughness, modeled basal drag, and sub-bed geology at this location on the glacier, but there is no corresponding change in the nature of the sediments immediately beneath the ice-bed interface. This synthesis is summarized in Figure 10 and Table 1.

## 4. Discussion: Ice Stream Dynamics and Subglacial Geology

### 4.1. Structure

[23] Beneath this part of the glacier, a major geological boundary separates sedimentary strata to the north, from basement rocks to the south. Covering these is a continuous

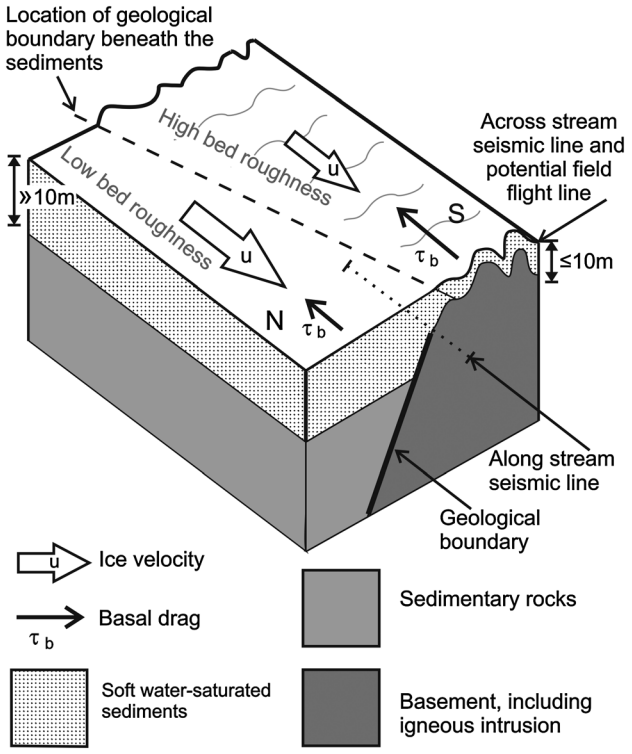


**Figure 10.** Schematic of synthesized subglacial interpretation from the area of the seismic surveys. Arrow lengths for ice velocity and basal drag indicate relative magnitudes.

**Table 1.** Synthesis of Interpreted Geophysical Measurements Relative to Interpreted Geological Boundary

| Measured Parameter | Change Across Geological Boundary (N to S) | Quantify Change |
|---|---|---|
| Ice velocity | Decrease | 325 to 290 m $a^{-1}$ |
| Basal drag | Increase | 3.4 to 7.8 kPa |
| Bed roughness | Increase | $\sigma = 3.4$ to $\sigma = 13.5$ m |
| Sediment acoustic impedance | No significant change | No change (mean = $2.9 \times 10^6$ kg $m^2$ $s^{-1}$) |
| Sediment thickness | Decrease | $\gg 10$ to $\leq 10$ m |
| Potential field (gravity and magnetic) | Yes | Sedimentary basin to basement rocks |

layer of soft, low-density, water-saturated sediments; these show no change in acoustic properties that coincide with the geological boundary beneath. However, a number of other parameters do show changes coincident with the boundary; from north to south, the upper surface of the soft sediments shows an increase in roughness (~300%), the modeled basal drag increases (>100%), and the flow speed of the ice decreases (11%).

### 4.2. Soft Sediment Thickness

[24] The thickness of the soft sediments is difficult to determine. To the south of the geological boundary, the acoustic impedance indicates their presence, but they are sufficiently thin that the upper surface of the basement rocks cannot be resolved. The seismic wavelength ($\lambda$) in the sediments is ~10–20 m; hence, we assume that they are of the order of up to 10 m thick ($\lambda/2$). The geological boundary dips steeply (4°) to the NW, juxtaposing basement rocks against the soft sediments and deeper sedimentary rocks (Figure 10). To the north of the boundary, there are no coherent reflections within 100 m depth of the bed (Figure 7), which suggests that the soft sediments are significantly thicker than they are to the south of the boundary (i.e., $\gg$10 m). The sediment density we interpret from both the seismic and gravity data is the same, which also suggests that north of the boundary, this material is much thicker and extends from the ice-bed interface right down to the bottom of the sedimentary basin (i.e., >500 m; Figure 8). Hence, our data indicate that north of the boundary the soft sediment layer is much thicker and perhaps nourished from the sedimentary basin beneath. There is thus a sufficient sediment thickness to smooth out the potential effects of any bedrock roughness on the ice-sediment interface. In contrast, to the south the soft sediment layer is thinner, allowing any roughness in the underlying basement rock to influence the flow of the overlying ice and be reflected in increased roughness and basal friction. This interpretation is summarized in Figure 10.

### 4.3. Basal Drag

[25] Although there is evidence elsewhere that sediment acoustic impedance is related to basal drag [*Vaughan et al.*, 2003], here there is no clear relationship; there is no significant change in impedance that corresponds with that seen in all the other parameters across the geological boundary. Whilst the presence of soft, water-saturated sediments is a requirement for fast ice flow, on PIG it is the deeper geology that appears to control the spatial variability in the flow. This control appears to operate through the basal sediment layer without having a significant impact on its acoustic properties, but is reflected in the ice-sediment interface roughness. This observation likely reflects particular properties (i.e., viscosity) of the basal sediment. Rheological modeling offers the best prospect for further investigation of this hypothesis.

[26] Our basal roughness was derived from the across-stream seismic line. The along-stream bed profile, which overlies the thicker soft-sediment layer, is smooth ($\sigma = 0.7$ m when a 1 km running mean is subtracted), consistent with this part of the across-stream line. With no corresponding profile in the rougher area to the south, it is not possible to be certain that there is a higher roughness along-stream there, but even the across-stream roughness increase will still most likely contribute to an enhanced basal drag.

[27] The northernmost area of low density sediment inferred from our gravity model (Figure 8), where we have no seismic data, also lies beneath a tributary of PIG and the velocity contour line we use to delineate the ice stream skirts around this feature (Figure 2c). It is possible that this thick sediment has a similar local effect on ice stream velocity, reducing basal friction and facilitating faster ice flow.

### 4.4. Subglacial Erosion

[28] Subglacial erosion removes substrate from beneath a glacier, transferring it further downstream. Where the bed consists of soft, poorly lithified sediments, this mechanism can be particularly rapid, even up to the order of meters per year [*Björnsson*, 1996; *Motyka et al.*, 2006; *Smith et al.*, 2007], and it is possible that eventually the complete removal of one subglacial layer, revealing a different lithology to outcrop beneath the ice, could have a significant effect on the ice flow regime. A comparison between surface elevation, ice thickness, and gravity measurements acquired recently [*Smith et al.*, 2012] and in 1961 [e.g., *Shimizu*, 1964], at a location ~50 km further downstream on PIG, shows the erosion of 32 m of bed sediments over a 49 year period [*Smith et al.*, 2012]. Our proposed thin subglacial sediment layer south of the geological boundary could indicate that prolonged erosion has almost, yet not quite completely removed the soft sediment there, and harder basement rocks are now not far below the ice-bed interface. If so, it is possible that continuing erosion will exhaust the sediment, bringing ice and basement into contact with each other. If this hypothesis is correct, it raises the possibility that the ice flow in this part of PIG could change as a result of evolving subglacial geology. We expect that basement rocks would ultimately impose a greater restraint on ice flow than the existing soft sediments, implying that basal drag would increase, reducing the ice velocity. Assuming a soft-sediment thickness south of the boundary of ~10 m, and a range of possible erosion rates between those traditionally expected in this environment and the high rates seen further downstream (~0.1–1 m $a^{-1}$), such a change could be initiated in 10–100 years. An alternative hypothesis would be one of steady state, in which sediments transported with the glacier are sufficient to replenish any removed by erosion, sustaining the fast ice flow. Repeat surveys over a prolonged period (years-decades) would be required to distinguish between these two hypotheses.

**Table 2.** Geophysical Methods and Resulting Components of the Combined Interpretation

| Method | Interpretation Components |
|---|---|
| Seismic—acoustic impedance | Presence of soft sediments across the whole line |
| | No significant change in acoustic properties |
| Seismic—topography | Bed roughness |
| | Soft sediment thickness |
| | Geological boundary |
| Gravity | Geological boundary |
| | Low density sedimentary basins |
| Magnetics | Igneous intrusion at very shallow depth below the bed |
| | Geological boundary |
| GPS | Ice flow speed |
| Modeling [*Morlighem et al*., 2010] | Basal drag |

[29] Elsewhere in West Antarctica, ice stream onset regions and trunks have been found to overlie a widespread, thick sediment layer with no evidence for basement rocks [e.g., *Smith*, 1997c; *Peters et al*., 2006; *King et al*., 2007]. Our interpretation is the first evidence for the presence of crystalline rocks close to the ice-bed interface in the upstream region of a modern Antarctic ice stream. This supports the findings from offshore studies of paleo-ice streams [e.g., *Lowe and Anderson*, 2003; *Larter et al*., 2009; *Graham et al*., 2009] which suggest former streaming flow over some areas of crystalline rock with only a thin layer of sediment or meltwater present.

## 5. Conclusions

[30] We have used a synthesis of multiple geophysical and glaciological data types (Table 2) to determine the relationship between ice dynamics and the underlying geology on Pine Island Glacier (Figure 10). Immediately beneath the ice is a layer of soft water-saturated sediment, overlying deeper, harder rocks which contain a significant geological boundary. Crossing the location of the boundary from north to south, the ice velocity decreases (by 11%), whilst bed roughness and modeled basal drag [*Morlighem et al*., 2010] both increase (by ~300% and >100%, respectively). The acoustic impedance of the soft sediments at the ice-bed interface shows no significant change across the boundary.

[31] The boundary appears to be a major transition in the deeper geology (i.e., beneath the soft sediments), dipping to the NW and separating a sedimentary basin north of the boundary from crystalline basement rocks to the south. We infer this is part of a major tectonic boundary underlying the main trunk of PIG and that a Cenozoic rift-related intrusion was emplaced along it. Two areas of low density sediments have been identified to the north of the tectonic boundary. One sedimentary basin is beneath the central flow region on the main trunk of PIG and another lies beneath an adjacent, slower-flowing tributary.

[32] The structure we interpret to the south of the geological boundary, namely a thin (~10 m) soft sediment layer between ice and underlying basement, has not been identified before beneath a contemporary Antarctic ice stream and this would not have been possible without both the seismic and the potential field data. Taken independently, the seismic data would have shown only the soft sediments, whereas the potential field data would have suggested ice in direct contact with the basement rocks. The joint interpretation, combined with the ice velocity, bed roughness, and basal drag results (Table 2), suggests an interaction between the deeper geology and the ice flow. Furthermore, in conjunction with the interpreted structure to the north of the boundary, this potentially forms a unique natural experiment that could indicate the impacts of subglacial erosion on ice flow.

[33] We believe the geological boundary and coincident change in basal roughness exert an important control on the flow regime of PIG. The smoother ice stream bed to the north, over the thicker sediments, appears to facilitate the fastest flow. The bed gets rougher to the south where the soft sediment layer beneath the ice is very thin over the area of basement rocks. We propose that the rough surface of the basement rocks to the south of the boundary increases the basal drag on the ice, through the intervening soft sediment. The validity of this proposal could most likely be investigated with modeling, which might indicate the rheological properties of the sediments.

[34] The high erosion rates observed further downstream [*Smith et al*., 2012] lead us to prefer a hypothesis that the soft sediment layer south of the boundary is being progressively eroded. This would imply that erosion has almost removed this sediment layer and that further erosion could finally exhaust it. Hence, the underlying basement rocks may soon outcrop beneath the ice, potentially increasing basal drag and reducing the ice flow. Repeat measurements on decadal time scales could indicate whether or not this, or the alternative steady state hypothesis, is correct.

[35] Another consequence of the eventual exposure of the basement rocks beneath the ice would be its effect on the resulting sedimentation record. Considering the ice flow and subglacial hydraulic gradients, any subglacially eroded material is most likely to be transported downstream and may become incorporated into the offshore sedimentary sequence deposited beyond the glacier, in Pine Island Bay. Provided the existing sediment layer is not till originally re-worked from the same basement rocks, a change in the eroded material type should eventually be reflected within this depositional sequence. How soon this could be detected following the future change in bed type we propose is hard to predict but it does raise the possibility that earlier, similar events may already be present in offshore sediments. High-resolution provenance studies of the Holocene parts of existing sediment cores from Pine Island Bay [e.g., *Lowe and Anderson*, 2002; *Ehrmann et al*., 2011] would be one way of investigating this possibility. Subglacial erosion has already been considered as a possible explanation for deeper changes in some of these cores [*Ehrmann et al*., 2011]. Although early Holocene ice-divide migration was actually the preferred conclusion of that study, any shallower evidence in the cores indicating recent subglacial erosion would support our interpretation of the present-day basal processes.

[36] Our combined interpretation of seismic and potential field data shows correlations between subglacial geological variations and variability in the flow of the overlying ice stream. This is the first time such data sets have been jointly interpreted to investigate subglacial conditions and have shown the influence of subglacial geology on ice flow to an unexpected level of detail. Similar studies elsewhere would indicate to what degree these results are typical of

polar ice streams, or limited to specific locations with particular geological configurations. We conclude that in general, an understanding of the shallow-medium depth subglacial geology beneath fast-flowing glaciers and ice streams is one of the essential components required to enable reliable predictions of future ice sheet behavior.

[37] **Acknowledgments.** Julian Scott made considerable contributions to all aspects of this work. This study is part of the British Antarctic Survey (BAS) programme Polar Science for Planet Earth. We thank NERC Geophysical Equipment Facility (Loan 847), BAS Operations and pilot David Leatherdale for supporting the data acquisition, C. Griffiths and F. Buckley for field assistance, and M. E. Morlighem for providing model results. We are grateful for discussions with Claus-Dieter Hillenbrand and for reviews by John Behrendt, Marta Ghidella, and two anonymous reviewers.

## References

Anandakrishnan, S., D. D. Blankenship, R. B. Alley, and P. L. Stoffa (1998), Influence of subglacial geology on the position of a West Antarctic ice stream from seismic observations, *Nature*, *394*, 62–65.

Atre, S. R., and C. R. Bentley (1993), Laterally varying basal conditions beneath ice streams B and C, West Antarctica, *J. Glaciol.*, *39*, 507–514.

Bamber, J. L., F. Ferraccioli, I. Joughin, T. Shepherd, D. M. Rippin, M. J. Siegert, and D. G. Vaughan (2006), East Antarctic ice stream tributary underlain by major sedimentary basin, *Geology*, *36*, 33–36, doi:10.1130/G22160.1.

Bamber, J. L., J. L. Gomez-Dans, and J. A. Griggs (2009), A new 1 km digital elevation model of the Antarctic derived from combined satellite radar and laser data—Part 1: Data and methods, *Cryosphere*, *3*, 101–111.

Bamber, J. L., D. G. Vaughan, and I. Joughin (2000), Widespread complex flow in the interior of the Antarctic ice sheet, *Science*, *287*, 1248–1250, doi:10.1126/science.287.5456.1248.

Behrendt J. C., D. D. Blankenship, C. A. Finn, R. E. Bell, R. E. Sweeney, S. M. Hodge, and J. M. Brozena (1994), CASERTZ aeromagnetic data reveal late Cenozoic flood basalts(?) in the West Antarctic rift system, *Geology*, *22*, 527–530.

Bell, R. E., D. D. Blankenship, C. A. Finn, D. L. Morse, T. A. Scambos, J. M. Brozena, and S. M. Hodge (1998), Influence of subglacial geology on the onset of a West Antarctic ice stream from aerogeophysical observations, *Nature*, *394*, 58–62.

Bentley, C. R. (1971), Seismic evidence for moraine within the basal Antarctic ice sheet, *Antarct. Res. Ser., 16*, edited by Crary, A. P., 89–129, AGU, Washington D.C.

Bentley, C. R., and H. Kohnen (1976), Seismic refraction measurements of internal friction in Antarctic ice, *J. Geophys. Res.*, *81*, 1519–1526.

Bingham, R. G., and M. J. Siegert (2009), Quantifying subglacial bed roughness in Antarctica: Implications for ice-sheet dynamics and history, *Quat. Sci. Rev.*, *28*, 223–236. doi:10.1016/j.quascirev.2008.10.014.

Bingham, R. G., F. Ferraccioli, E. C. King, R. D. Larter, H. D. Pritchard, A. M. Smith, and D. G. Vaughan (2012), Inland thinning of West Antarctic Ice Sheet steered along subglacial rifts, *Nature*, *487*, 469–471, doi:10.1038/nature11292.

Björnsson, H. (1996), Scales and rates of glacial sediment removal: A 20 km long, 300 m deep trench created beneath Breidamerkurjokull during the little Ice Age, *Ann. Glaciol.*, *22*, 141–146.

Brockamp, B., and H. Kohnen (1965), Ein Beitrag zu den seismischen Untersuchungen auf dem Groenlandischen Indandeis, *Polarforschung*, *6*, 2–12.

Ehrmann, W., C.-D. Hillenbrand, J. A. Smith, A. C. G. Graham, G. Kuhn, and R. D. Larter (2011), Provenance changes between recent and glacial-time sediments in the Amundsen Sea embayment, West Antarctica: Clay mineral assemblage evidence, *Ant. Sci.*, *23*, 471–486.

Ferraccioli, F., M. Gambetta, and E. Bozzo (1998), Microlevelling procedures applied to regional aeromagnetic data: An example from the Transantarctic Mountains (Antarctica), *Geophysical Prospecting*, *46*, 177–196.

Ferraccioli, F., E. Bozzo, and D. Damaske (2002), Aeromagnetic signatures over western Marie Byrd Land provide insight into magmatic arc basement, mafic magmatism and structure of the Eastern Ross Sea Rift flank, *Tectonophysics*, *347*, 139–165, doi: 10.1016/S0040-1951(01)00242-6.

Ferraccioli, F., and E. Bozzo (2003), Cenozoic strike-slip faulting from the eastern margin of the Wilkes Subglacial Basin to the western margin of the Ross Sea Rift: An aeromagnetic connection, in *Intraplate Strike-slip Deformation, Special Publication*, vol. *210*, edited by F. Storti, R. E. Holdsworth, and F. Salvini, pp. 109–133, Geological Society, London.

Ferraccioli, F., T. A. Jordan, D. G. Vaughan, J. W. Holt, P. R. James, H. Corr, D. D. Blankenship, J. D. Fairhead, and T. M. Diehl (2007a), New aerogeophysical survey targets the extent of the West Antarctic Rift System over Ellsworth Land, in *Antarctica: A Keystone in a Changing World—Online Proceedings for the 10th International Symposium on Antarctic Earth Sciences*, edited by A. Cooper, C. Raymond et al., U.S. Geological Survey Open-File Report 2007-1047, Extended Abstract 113 (http://pubs.usgs.gov/of/2007/1047/).

Ferraccioli, F., T. Jordan, E. Armadillo, E. Bozzo, H. Corr, G. Caneva, C. Robinson, N. Frearson, and I. Tabacco (2007b), Collaborative aerogeophysical campaign targets the Wilkes Subglacial Basin, the Transantarctic Mountains and the Dome C region. In: Bozzo, E., Ferraccioli, F. (Eds.), The Italian–British Antarctic Geophysical and Geological Survey in Northern Victoria Land 2005–06—Towards the International Polar Year 2007–08, *Terra Antartica Reports*, vol. *13*, pp. 1–36.

Ferraccioli, F., A. Armadillo, T. A. Jordan, E. Bozzo, and H. Corr (2009), Aeromagnetic exploration over the East Antarctic ice sheet: A new view of the Wilkes Subglacial Basin, *Tectonophysics*, *478*, 62–77.

Graham, A. G. C., R. D. Larter, K. Gohl, C.-D. Hillenbrand, J. A. Smith, and G. Kuhn (2009), Bedform signature of a West Antarctic palaeo-ice stream reveals a multi-temporal record of flow and substrate control, *Quaternary Sci. Rev.*, *28*, 2774–2793, doi:10.1016/j.quascirev.2009.07.003.

Holland, C. W., and S. Anandakrishnan (2009), Subglacial seismic reflection strategies when source amplitude and medium attenuation are poorly known, *J. Glaciol.*, *55*, 931–937, doi:10.3189/002214309790152528.

Holt, J. W., D. D. Blakenship, D. L. Morse, D. A. Young, M. E. Peters, S. D. Kempf, T. G. Richter, D. G. Vaughan, and H. F. J. Corr (2006), New boundary conditions for the West Antarctic Ice Sheet: Subglacial topography of the Thwaites and Smith glacier catchments, *Geophys. Res. Lett.*, *33*, L09502, doi:10.1029/2005GL025561.

Jordan, T. A., F. Ferraccioli, D. G. Vaughan, J. W. Holt, H. Corr, D. D. Blankenship, and T. M. Diehl (2010), Aerogravity evidence for major crustal thinning under the Pine Island Glacier region (west Antarctica), *Geol. Soc. Am. Bull.*, doi:10.1130/B26417.1.

Jordan, T. A., F. Ferraccioli, N. Ross, H. F. J. Corr, P. T. Leat, R. G. Bingham, D. M. Rippin, A. le Brocq, M. J. Siegert (2012), Inland extent of the Weddell Sea Rift imaged by new aerogeophysical data, *Tectonophysics*, doi:10.1016/j.tecto.2012.09.010.

Joughin, I., E. Rignot, C. E. Rosanova, B. K. Luccita, and J. Bohlander (2003), Timing of recent accelerations of Pine Island Glacier, Antarctica, *Geophys. Res. Lett.*, *30*, 1706, doi:10.1029/2003GL017609.

Joughin, I., S. Tulaczyk, J. L. Bamber, D. Blankenship, J. W. Holt, T. Scambos, and D. G. Vaughan (2009), Basal conditions for Pine Island and Thwaites Glaciers, West Antarctica, determined using satellite and airborne data, *J. Glaciol.*, *55*, 245–257, doi:10.3189/002214309788608705.

King, E. C., J. Woodward, and A. M. Smith (2004), Seismic evidence for a water-filled canal in deforming till beneath Rutford Ice Stream, West Antarctica, *Geophys. Res. Lett.*, *31*, L20401, doi:10.1029/2004GL020379.

King, E. C., J. Woodward, and A. M. Smith (2007), Seismic and radar observations of subglacial bed forms beneath the onset zone of Rutford Ice Stream Antarctica, *J. Glaciol.*, *53*, 665–672, doi:10.3189/002214307784409216.

Kirchner, J. F., and C. R. Bentley (1990), Seismic short-refraction studies using an analytical curve-fitting technique, *Antarct. Res. Ser.*, *42*, 109–126.

Ku, C. C., and J. A. Sharp (1983), Werner deconvolution for automated magnetic interpretation and its refinement using Marquardt inverse modeling, *Geophysics*, *48*, 754–774, doi:10.1190/1.1441505.

Larter, R. D., A. G. C. Graham, K. Gohl, G. Kuhn, C.-D. Hillenbrand, J. A. Smith, T. J. Deen, R. A. Livermore, and H.-W. Schenke (2009), Subglacial bedforms reveal complex basal regime in a zone of paleo-ice stream convergence, Amundsen Sea Embayment, West Antarctica, *Geology*, *37*, 411–414, doi:10.1130/G25505A.1.

Li, X., B. Sun, M. J. Siegert, R. G. Bingham, X. Tang, D. Zhang, X. Cui, and X. Zhang (2010), Characterization of subglacial landscapes by a two-parameter roughness index, *J. Glaciol.*, *56*, 831–836.

Lowe, A. L., and J. B. Anderson (2002), Reconstruction of the West Antarctic ice sheet in Pine Island Bay during the Last Glacial Maximum and its subsequent retreat history, *Quat. Sci. Rev.*, *21*, 1879–1897.

Lowe, A. L., and J. B. Anderson (2003), Evidence for abundant subglacial meltwater beneath the paleo-ice sheet in Pine Island Bay, Antarctica, *J. Glaciol.*, *49*, 125–138.

Morlighem, M., E. Rignot, H. Seroussi, E. Larour, H. Ben Dhia, and D. Aubry (2010), Spatial patterns of basal drag inferred using control methods from a full-Stokes and simpler models for Pine Island Glacier, West Antarctica, *Geophys. Res. Lett.*, *37*, L14502, doi:10.1029/2010GL043853.

Motyka, R. J., M. Truffer, E. M. Kuriger, and A. K. Bucki (2006), Rapid erosion of soft sediments by tidewater glacier advance: Taku Glacier, Alaska, USA, *Geophys. Res. Lett.*, *33*, L24504, doi:10.1029/2006GL028467.

Peters, L. E., S. Anandakrishnan, R. B. Alley, J. P. Winberry, D. E. Voigt, A. M. Smith, and D. L. Morse (2006), Subglacial sediments as a control on the onset and location of two Siple Coast ice streams, West Antarctica, *J. Geophys. Res.*, *111*, B01302, doi:10.1029/2005JB003766.

Pilkington, M., and B. J. Thurston (2001), Draping corrections for aeromagnetic data: Line versus grid-based approaches, *Explor. Geophys.*, *32*, 95–101.

Rignot, E. (1998), Fast recession of a West Antarctic glacier, *Science*, *281*, 549–551, doi:10.1126/science.281.5376.549.

Rignot, E. (2008), Changes in West Antarctic ice stream dynamics observed with ALOS PALSAR data, *Geophys. Res. Lett.*, *35*, L12505, doi:10.1029/2008GL033365.

Rignot, E., J. L. Bamber, M. R. van den Broeke, C. Davis, Y. Li, W. J. van de Berg, and E. V. Meijgaard (2008), Recent Antarctic ice mass loss from radar interferometry and regional climate modeling, *Nat. Geosci.*, *1*, 106–110, doi:10.1038/ngeo102.

Rignot, E., D. G. Vaughan, M. Schmeltz, T. Dupont, and D. MacAyeal (2002), Acceleration of Pine Island and Thwaites Glaciers, West Antarctica, *Ann. Glaciol.*, *34*, 189–194.

Rippin, D. M., D. G. Vaughan, and H. F. J. Corr (2011), The basal roughness of Pine Island Glacier, West Antarctica, *J. Glaciol.*, *57*, 67–76.

Robin G. deQ (1958), Glaciology III, seismic shooting and related investigations, *Norw. Br. Swed. Antarc. Exped., 1949-1951, 5*, Norsk Polarinstitut, Oslo, Norway.

Roethlisberger, H. (1972), Seismic exploration in cold regions, CRREL Monograph II-A 2a 139 pp.

Scott, J. B. T., G. H. Gudmundsson, A. M. Smith, R. G. Bingham, H. D. Pritchard, and D. G. Vaughan (2009), Increased rate of acceleration on Pine Island Glacier strongly coupled to changes in gravitational driving stress, *Cryosphere*, *3*, 125–131.

Shepherd, A., D. J. Wingham, J. A. D. Mansley, and H. F. J. Corr (2001), Inland thinning of Pine Island Glacier, West Antarctica, *Science*, *291*, 862–864, doi:10.1126/science.291.5505.862.

Shepherd, T., J. L. Bamber, and F. Ferraccioli (2006), Subglacial geology in Coats Land, East Antarctica, revealed by airborne magnetic and radar sounding, *Earth Planet. Sc. Lett.*, *244*, 323–335, doi:10.1016/j.epsl.2006.01.068.

Shimizu, H, (1964), Glaciological studies in West Antarctica, 1960–1962, in *Antarctic Snow and Ice Studies, Antarctic Res. Ser*., vol. *2*, 37–64, AGU, Washington, D.C.

Smith, A. M. (1997a), Basal conditions on Rutford Ice Stream, West Antarctica, from seismic observations, *J. Geophys. Res.*, *102*, 543–552.

Smith, A. M. (1997b), Seismic investigations on Rutford Ice Stream, West Antarctica, PhD thesis, The Open University, United Kingdom, p. 127.

Smith, A. M. (1997c), Variations in basal conditions on Rutford Ice Stream, West Antarctica, *J. Glaciol.*, *43*, 245–255.

Smith, A. M. (2007), Subglacial bed properties from normal-incidence seismic reflection data, *J. Environ. Eng. Geophys*, *12*, 3–13.

Smith, A. M., and T. Murray (2009), Bedform topography and basal conditions beneath a fast-flowing West Antarctic ice stream, *Quat. Sci. Rev.*, *28*, 584–596, doi:10.1016/j.quascirev.2008.05.010.

Smith, A. M., T. Murray, K. W. Nichols, K. Makinson, G. Aðalgeirsdóttir, and A. E. Behar (2007), Rapid erosion drumlin formation and changing hydrology beneath an Antarctic ice stream, *Geology*, *35*, 127–130, doi:10.1103/G23036A.

Smith, A. M., C. R. Bentley, R. G. Bingham, and T. A. Jordan (2012), Rapid subglacial erosion beneath Pine Island Glacier, West Antarctica, *Geophys. Res. Lett.*, *39*, L12501, doi:10.1029/2012GL051651.

Telford, W. M., L. P. Geldart, and R. E. Sheriff (1990), *Applied Geophysics*, 2nd ed., Cambridge University Press, Cambridge, United Kingdom.

Vaughan, D. G., and R. Arthern (2007), Why is it hard to predict the future of ice sheets? *Science*, *315*, 1503–1504, doi:10.1126/science.1141111.

Vaughan, D. G., A. M. Smith, H. F. J. Corr, A. Jenkins, C. R. Bentley, M. D. Stenoien, S. S. Jacobs, T. B. Kellogg, E. J. Rignot, and B. K. Luchitta (2001), A review of the ice-sheet dynamics in the Pine Island Glacier basin, West Antarctica: Hypotheses of instability vs. Observations of change, in *The West Antarctic Ice Sheet: Behavior and Environment, Antarct. Res. Ser*., vol. *77*, edited by R. B. Alley, and R. A. Bindschadler, pp. 237–256, AGU, Washington, D. C.

Vaughan, D. G., A. M. Smith, P. C. Nath, and E. Le Meur (2003), Acoustic impedance and basal shear stress beneath four Antarctic ice streams, *Ann. Glaciol.*, *36*, 225–232.

Vaughan, D. G., H. F. J. Corr, F. Ferraccioli, N. Frearson, A. O'Hare, D. Mach, J. W. Holt, D. D. Blankenship, D. L. Morse, and D. A. Young (2006), New boundary conditions for the West Antarctic ice sheet: Subglacial topography beneath Pine Island Glacier, *Geophys. Res. Lett.*, *33*, L09501, doi:10.1029/2005GL025588.

Wingham, D. J., D. W. Wallis, and A. Shepherd (2009), Spatial and temporal evolution of Pine Island Glacier thinning, 1995-2006, *Geophys. Res. Lett.*, *36*, L17501, doi:10.1029/2009GL039126.